Deposition of Functional Organic Thin Films by Pulsed Plasma Polymerization: A Joint Theoretical and Experimental Study

Laurent Denis, Philippe Marsal, Yoann Olivier, Thomas Godfroid, Roberto Lazzaroni, Michel Hecq, Jérôme Cornil,* Rony Snyders

The pulsed plasma polymerization of allylamine and cyclopropylamine is investigated to study the influence of the precursor chemical structure on the process selectivity toward the primary amine groups. Both systems are compared under similar mean powers injected in the discharges (P_{mean}). The results reveal an increase in the precursor fragmentation in the plasma and a decrease in the primary amine content of the film (%NH_2) as P_{mean} increases. Nevertheless, below a critical P_{mean} value, different behaviors are observed depending on the precursor, cyclopropylamine being less plasma-fragmented than allylamine. As a result, plasma polymer films (PPF) synthesized from cyclopropylamine yield the largest %NH_2. These results are rationalized with the help of theoretical calculations pointing to a preferential opening of the cyclopropylamine ring structure. Cyclopropylamine activation in the plasma can thus be achieved without fragmentation reactions, leading to a more efficient incorporation of the $-NH_2$ group of the precursor in the PPF.

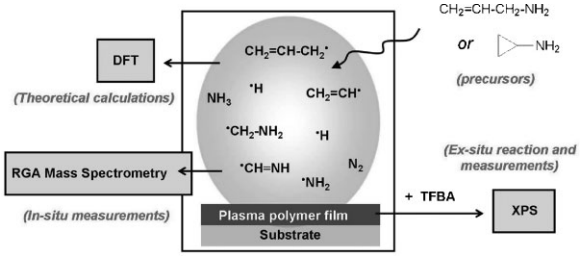

Introduction

Plasma polymerization is a very attractive technology for material surface modification through the deposition of organic thin films. The deposits, referred to as plasma polymer films (PPFs), result from the plasma activation of an organic precursor mainly via electron impact (EI) collisions. This solvent-free method provides thin films with good adhesion on many substrates such as polymers, glasses, ceramics, and metals.[1] PPF are not characterized by repeating monomer units as conventional polymer materials but exhibit an intrinsic crosslinked structure resulting from the large variety of precursor chemical bond dissociation processes that occur in the plasma.[2] The crosslinked structure triggers interesting properties such as excellent mechanical resistance and thermal stability.[3–5] This technology allows for the use of an exceptionally wide range of chemical precursors. Virtually any volatile compound including saturated ones can be used, offering numerous strategies for surface modification. However, despite the abundant literature related to such surface modification processes, plasma polymerization remains unclear in many aspects, in particular in the understanding of the relationship between plasma chemistry and PPF characteristics.

J. Cornil, P. Marsal, Y. Olivier, R. Lazzaroni
Service de Chimie des Matériaux Nouveaux, Université de Mons, Place du Parc 20, B-7000 Mons, Belgium
Fax: (+32) 0 65 37 38 61; E-mail: jerome@averell.umh.ac.be
L. Denis, M. Hecq, R. Snyders
Laboratoire de Chimie Inorganique et Analytique, Université de Mons, Place du Parc 20, B-7000 Mons, Belgium
T. Godfroid, R. Lazzaroni, M. Hecq, R. Snyders
Materia Nova Research Center, Parc Initialis, Avenue N. Copernic 1, B-7000 Mons, Belgium

Plasma Process. Polym. **2010**, *7*, 172–181

DOI: 10.1002/ppap.200900131

Since electrons are the lightest particles in the plasma, they absorb the largest amount of energy injected in the discharge. Typically, their average kinetic energy ranges between 2 and 5 eV. This energy can be transferred via collisions to the gas molecules leading to activation, dissociation, and ionization processes. It is worth distinguishing here activation versus dissociation processes; activation refers to the generation of radical species and involves breaking of chemical bonds of the precursor, but not necessarily its fragmentation such as in dissociation reactions. Since the ionization threshold of organic molecules (≈9–13 eV) is much higher than the energy of their chemical bonds (≈3–4 eV),[6] free radical concentration in the plasma is generally up to 10^5 times larger than the ion concentration.[6,7] Although it has been shown that positive ion-molecule reactions occurring in the plasma can have important influence in the PPF deposition process, especially if the plasma polymerization is carried out in CW mode at low input power to precursor flow rate ratios,[8–15] free radicals are herein considered to be the dominant species controlling the PPF growth by radical–molecule or radical–radical reactions.[6,7]

Initially, most of the studies related to plasma polymerization focused on the production of highly crosslinked PPF. Such PPF are obtained when a high level of precursor fragmentation is reached in the plasma. Therefore, high-energy conditions have usually been employed due to the precursor fragmentation dependence on the energy dissipated in the system.[2] Under such plasma conditions, as a result of extensive fragmentation reactions, various kinds of chemical functions all derived from the precursor molecule are incorporated in the PPF, thus leading to a poor chemical control of the PPF composition. During the last years, in view of its high potential for material surface modification, plasma polymerization has been further developed in the search for PPF with stable and selective chemistry.[16–18]

Based on these considerations, the pulsed plasma polymerization appears to be a very promising technique to enhance the controllability of the PPF chemistry due to a better control of the energy dissipation in the plasma. In pulsed conditions, the plasma is intermittently generated according to the pulse frequency; the so-called duty cycle (Δ) gives the relationship between the plasma on- and off-times (τ_{on}, time during which the plasma species are produced; τ_{off}, time during which the plasma is switched off).

$$\Delta = \tau_{on}/(\tau_{on} + \tau_{off}) \quad (1)$$

The mean power (P_{mean}) is then defined and represents the average energy dissipated in the plasma over the pulse period, with P_{peak} the power injected during τ_{on}.

$$P_{mean} = \Delta \times P_{peak} \quad (2)$$

Although the duty cycle has often been varied to control the retention in the PPF of the chemical group hosted by the chemical precursor,[16,19,20] it has been shown that P_{mean} is actually the key parameter to be modulated.[21–23]

Among the most promising PPF, primary amine-based films (NH_2-PPF) containing a high level of primary amine functions have received a great deal of interest in view of many potential applications ranging from modification of filtration membranes,[24–26] treatment of polymeric beads,[27,28] and carbon nanotubes[29] to biomedical applications.[18,19,21,30–34] Several nitrogen-rich precursors such as *n*-butylamine,[25] *n*-heptylamine,[30,35–37] ethylenediamine,[24,29,38] diaminocyclohexane,[39] 1,3-diaminopropane,[40] and propylamine[41,42] have been used for NH_2-PPF syntheses. Allylamine is, however, the most exploited.[18–23,25–28,31–34,41–48]

One of the major conclusions of recent works dealing with NH_2-PPF bioapplications is that the PPF biological response is noticeably enhanced when their primary amine content (%NH_2) is increased.[21,26] However, the understanding at a fundamental level of the relationship between the nature of the precursor, the fragmentation processes in the plasma, and %NH_2 is not straightforward to assess from all previous studies due to systematic changes in both chemical precursors (i.e., raw chemical formulae) and process conditions. This has motivated us to consider two isomeric precursors, namely allylamine and cyclopropylamine (C_3H_7N), so that the differences observed between the two systems, in similar experimental conditions, only result from differences in the precursor chemical structure.

To date, despite the abundant literature related to plasma polymerization, most of the works have been devoted to the chemical characterization of the PPF while little attention has been paid to the plasma chemistry frequently considered as a "black box." The originality of the present work dealing with pulsed plasma polymerization is to investigate the plasma-phase activation of allylamine and cyclopropylamine precursors and assess its impact on the PPF chemistry. Both experimental and theoretical approaches have been used to shed light into this process, with the additional objective to define a low-cost and fast screening protocol for testing the potentiality of other precursors. The plasma chemistry has been analyzed by residual gas analysis (RGA) mass spectrometry. The enthalpies of reaction of the precursor initial fragmentations have been calculated at the density functional theory (DFT) level in order to assist the interpretation of the mass spectra. The NH_2-PPF chemical composition has been

determined by X-ray photoelectron spectroscopy (XPS) combined with a chemical derivatization method using 4-trifluoromethyl-benzaldehyde (TFBA) as labeling molecule. With this approach, primary amine functions are directly probed following specific reaction with TFBA and quantified without the need of XPS photoelectron peak fitting. All together, our work unambiguously demonstrates that $\%NH_2$ can be increased through an appropriate choice of the precursor. Cyclopropylamine is found to yield a larger $\%NH_2$ compared to allylamine due to preferential bond breakings in the ring structure; the latter is not accompanied by a loss of the NH_2 functionality in contrast to the situation prevailing for allylamine.

Experimental Part

Materials and Methods

Allylamine and cyclopropylamine (98% purity), purchased from Acros Organics, have been plasma-polymerized on 1 cm^2 (100) silicon substrates. Prior to synthesis, substrates were ultrasonically washed in hexane and then rinsed with methanol.[23]

PPF syntheses were carried out in a cylindrical stainless steel vacuum chamber (diameter of 350 mm and height of 450 mm). A residual pressure of 8×10^{-7} Torr was reached by a combination of rotary and turbomolecular pumps connected in series. The 13.56 MHz exciting power was applied via a matching network to a water-cooled copper coil (150 mm internal diameter, 8 mm thick) located inside the chamber 100 mm in front of the substrate. A load-lock system allowed for transferring the substrate, fixed vertically on a substrate holder itself mounted on a transfer stick, inside the reactor from ambient atmosphere to high vacuum in a few minutes. The precursor flow rate was fixed at 10 standard cubic centimeters per minute (sccm) during all experiments and the working pressure regulated at 2.67 Pa. Allylamine- and cyclopropylamine-based PPF were synthesized with variations in the P_{mean} dissipated in the discharge from 8 to 60 W. Table 1 reports the experimental conditions employed in terms of P_{peak}, duty cycle, and pulse frequency. In the range of P_{mean} considered, allylamine and cyclopropylamine have very similar deposition rates which range from 3 to 50 $nm \cdot min^{-1}$ when PPF are synthesized between 8 and 60 W, respectively.

Table 1. Experimental conditions employed. The pulse frequency is fixed at 525 Hz, thus corresponding to a pulse period of 1.9 ms.

P_{mean}	P_{peak}	Duty cycle
W	W	%
8	40	20
12	40	30
16	40	40
30	150	20
45	150	30
60	150	40

The mass spectrometer, used to analyze the plasma composition through time-averaged measurements, was a quadrupole HAL EQP 500 model supplied by Hiden Analytical. The apparatus was connected to the chamber by a 100 μm extraction orifice located between the coil and substrate holder. Prior to detection, neutral species were ionized by EI with an electron kinetic energy fixed at 20 eV in order to limit additional fragmentations in the ion source.[7,49,50] We stress that the mass spectrometer quadrupole is a mass-dependent system whose transmission function strongly decreases with the studied mass, m. The manufacturer of the HAL EQP 500 model has found empirically that the mass-dependent instrument function evolves between m^{-1} and m^{-2}. In this work, we used an m^{-1} mass-dependent function to correct the spectra[15] but using m^{-2} would not change the main conclusions.

XPS experiments were performed on as-deposited and TFBA-derivatized samples. Data were acquired on a VG-ESCALAB 220iXL spectrometer. A monochromatized Al K_α line (1 486.6 eV) was used as a photon source. The pressure in the analysis chamber was typically 2×10^{-9} Torr. Surface charging effect was compensated for using a 6 eV electron flood gun. The photoemission spectrum background signal was subtracted using the linear method. Elemental composition was inferred from photoelectron peak areas using the respective photoionization cross-section calculated by Scofield[51] and corrected by the electron inelastic mean free path and the transmission function of the spectrometer analyzer.[52]

In XPS, the binding energy shifts associated with specific functional groups do not always give a precise function identification and quantification. For instance, nitrogen in a primary amine environment and nitrogen in a secondary or tertiary amine environment are not readily distinguishable from binding energy shifts.[53] In order to overcome this difficulty, one often uses a chemical reaction specific to the functional group of interest.[54–56] The idea is to employ a labeling molecule that introduces a tag atom not present in the sample prior to the reaction. In this work, the derivatization reaction was performed by exposing the PPF to TFBA vapor in a separated chamber (pumped to a residual pressure of 3 Pa) at 400 Pa pressure and room temperature. TFBA has been widely used for primary amine group derivatization;[23,39,57–61] the reaction consisted in a nucleophilic addition on a carbonyl group (C=O) that converts the NH_2 group into an imine function. A high selectivity toward primary amines can be reached with this reaction owing to the TFBA molecular structure. The obtained aromatic imine has its C=N bond conjugated to the C=C bonds of the aromatic cycle, thus making the system highly stable due to the π-electron delocalization (Scheme 1). The NH_2 groups were quantified by detecting the reagent CF_3 terminal groups. In a previous work, the time required to reach the complete derivatization reaction, considering an allylamine-based film synthesized at $P_{mean} = 30$ W, has been estimated to be around 16 h.[23] In the present study, since a higher $\%NH_2$ is expected, the reaction has been performed during

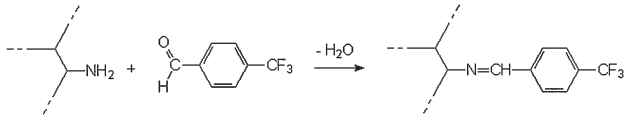

Scheme 1. Chemical gas-phase reaction between the PPF primary amines and TFBA.

Plasma Process. Polym. **2010**, *7*, 172–181

DOI: 10.1002/ppap.200900131

40 h. When investigating the process selectivity toward the incorporation of the primary amine group of the precursor in the PPF, $\%NH_2$ is ultimately calculated as:

$$\%NH_2 = \frac{[NH_2]}{[N]} = \frac{([F]/3)}{[N]} \times 100\% \quad (3)$$

where [N] and [F] are the relative concentrations of nitrogen and fluorine at the PPF surface, as determined by XPS measurements, respectively.

Results and Discussion

Mass Spectrometry

In a previous work focusing on the plasma polymerization of allylamine, we demonstrated that the amount of unfragmented chemical precursor remaining in the discharge is directly related to $\%NH_2$.[23] Prior investigating allylamine and cyclopropylamine plasma chemistry in similar P_{mean} conditions, the EI mass spectrum of each vapor has been recorded (Figure 1a, b). In these experiments, the plasma is switched off, the precursor flow rate fixed at 10 sccm and the pressure in the deposition chamber regulated at 2.67 Pa. The four peaks observed at *m/z* 57, 56, 30, and 28 result from α-cleavage reactions of the precursors ($[C_3H_7N]^{+\cdot}$) following their ionization in the mass spectrometer. This radical-cation (*m/z* 57) can lose either a hydrogen atom giving the ($[C_3H_6N]^+$) signal at *m/z* 56 or a vinyl radical producing the ($[CH_4N]^+$) signal at *m/z* 30. Subsequent dehydrogenation of the latter yields the ($[CH_2N]^+$) signal at *m/z* 28. Since the same *m/z* signals are detected, Figure 1a and b point to similar fragmentation patterns for both precursors during the ionization process. However, the variations in signal intensity suggest different ionization yields between allylamine and cyclopropylamine likely due to different ionization cross sections. This has to be taken into account for the comparison of both plasma chemistries. Accordingly, the intensity of the precursor mass signal measured in given P_{mean} conditions was normalized by its corresponding value in the EI spectrum (i.e., $I^{56}_{\text{plasma on}}/I^{56}_{\text{plasma off}}$, see Figure 2a). Throughout the text, the precursor mass signal refers to the most intense peak at *m/z* 56. On that basis, the differences observed in the RGA mass spectra (i.e., with the plasma on, see Figure 1c–f) are assigned to different fragmentation patterns of the precursors in the plasma.

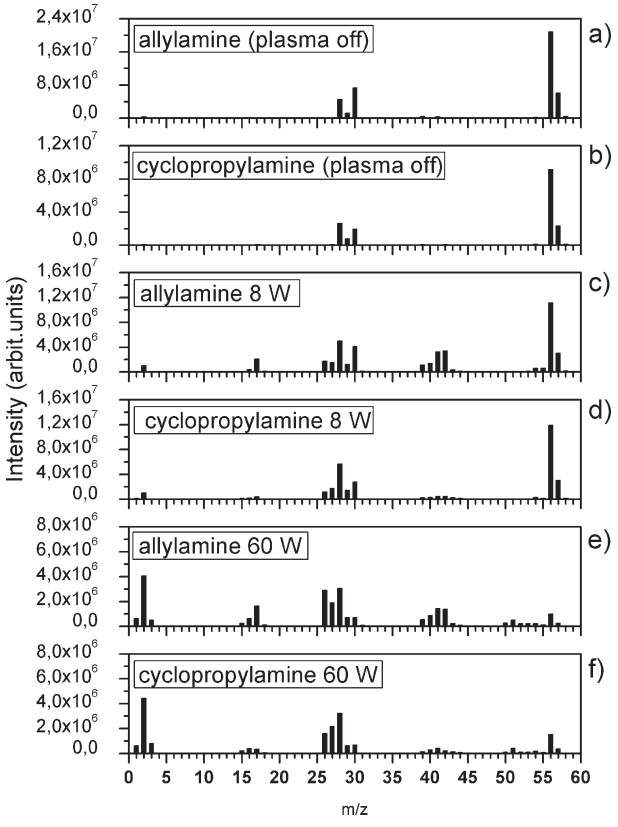

Figure 1. Electron impact (EI) mass spectra of allylamine (a) and cyclopropylamine (b). RGA mass spectra of allylamine (c and e) and cyclopropylamine (d and f) plasmas for two different P_{mean} values.

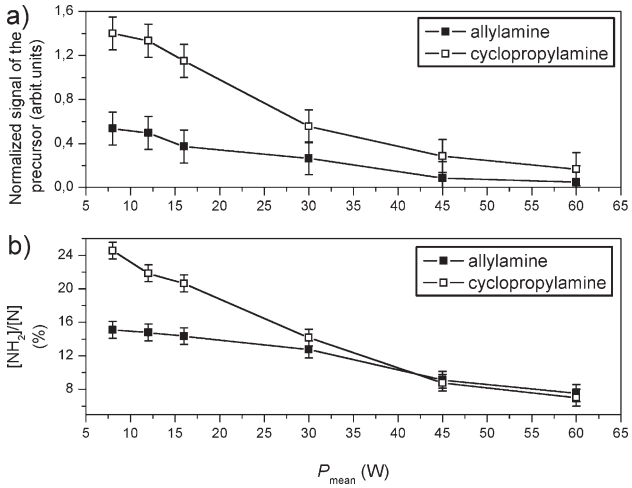

Figure 2. a) Normalized signal of both precursors in the plasma in relation to b) the primary amine content in the corresponding PPF when varying the P_{mean} conditions.

Figure 1c–f show the RGA mass spectra of allylamine and cyclopropylamine plasmas for the lowest (8 W) and highest (60 W) P_{mean} conditions. The different peaks were assigned as follows — *m/z* 1, 2, 3: ($[H_X]^+$) with *X* varying from 1 to 3; *m/z* 15, 16, 17, 18: ($[NH_X]^+$) with *X* ranging from 1 to 4 and a contribution from ($[CH_3]^+$), ($[CH_4]^{+\cdot}$), and ($[H_2O]^{+\cdot}$) at *m/z* 15, 16, and 18, respectively; *m/z* 26: ($[CN]^+$) and ($[C_2H_2]^{+\cdot}$); *m/z* 28: ($[CH_2N]^+$), ($[C_2H_4]^{+\cdot}$), and ($[N_2]^{+\cdot}$); *m/z* 30: ($[CH_4N]^+$) and ($[C_2H_6]^{+\cdot}$); *m/z* 41 and 42: ($[C_3H_5]^+$) and ($[C_3H_6]^{+\cdot}$), respectively. The mass signals observed below *m/z* 55 suggest that the chemical precursor can be highly

dehydrogenated in the plasma at low P_{mean} (8 W); signals between *m/z* 50 and 58 correspond to molecular fragments ($[C_3H_XN]^+$), with *X* varying from 0 to 8.

Figure 1c–f illustrate that many additional peaks appear in the RGA mass spectra of allylamine and cyclopropylamine plasmas compared to the EI mass spectra of the respective vapors (Figure 1a, b). Moreover, it is clearly observed that the precursors have quite different fragmentation patterns in the plasma. Cyclopropylamine appears to be plasma-fragmented in a more selective way than allylamine. As a matter of fact, the majority of the cyclopropylamine fragments are located around the *m/z* 2 and *m/z* 28 peaks while, for allylamine, fragments are distributed in a more homogeneous way, that is, in the *m/z* 2, *m/z* 16, *m/z* 28, and *m/z* 41 regions of the mass spectra. The two systems can also be distinguished with respect to the production of ammonia (signal at *m/z* 17) which is much more pronounced in the allylamine plasma. Moreover, the intensity of the NH_3 signal in the allylamine plasma is always more intense than the *m/z* 16 one (mostly related to the NH_2 radical and hence, to breaking of the C—N precursor bond).

Figure 2a shows the decrease in the normalized intensity of the mass signal of both precursors with increase in P_{mean}, pointing to an amplification of the fragmentation reactions. When compared, the mass signal of the precursors becomes similar (within the error bars) beyond a critical P_{mean} value of ≈30 W (P^c_{mean}). For $P_{mean} < P^c_{mean}$, different behaviors are clearly observed for the two precursors; the cyclopropylamine mass spectra are indicative of a larger amount of unfragmented precursor compared to allylamine. For $P_{mean} > P^c_{mean}$, the normalized mass signals of both precursors have similar intensities, thus suggesting that the plasma fragmentation occurs in a significant way though in similar proportions. These observations underline the existence of a P_{mean} threshold value under which the selectivity of the fragmentation processes in the plasma can be controlled by acting on the precursor chemical structure. In contrast, when the plasma conditions are above this threshold, the process does not show any selectivity toward a given precursor.

From these mass spectrometry measurements, it is expected from ref.[23] that, when $P_{mean} < P^c_{mean}$, PPF synthesized from cyclopropylamine have a larger $\%NH_2$ than films made from allylamine. For $P_{mean} > P^c_{mean}$, PPF synthesized from either precursor should yield a similar $\%NH_2$ due to the loss of the process selectivity in terms of precursor fragmentation.

X-ray Photoelectron Spectroscopy (XPS)

Table 2 collects the chemical composition of the as-deposited and TFBA-derivatized PPF based on allylamine versus cyclopropylamine. Each sample contains a few percents of oxygen though both precursors are free of this element. This is explained by the substantial amount of free radicals that are trapped in the PPF network during their

Table 2. Elemental composition of the allylamine- and cyclopropylamine-based PPF before and after the derivatization reaction as a function of the P_{mean} conditions.

Precursor type	P_{mean}	Elemental composition of the PPF						
	W	As-deposited			TFBA-derivatized			
		[C]	[N]	[O]	[C]	[N]	[O]	[F]
Allylamine	8	73.6	24.7	1.7	71.2	17.7	3.1	8.0
	12	74.6	24.4	1.0	70.8	17.8	3.5	7.9
	16	75.5	23.4	1.1	72.4	16.9	3.4	7.3
	30	77.0	21.1	1.9	74.8	16.3	2.7	6.2
	45	79.2	19.7	1.1	78.3	15.3	2.2	4.2
	60	81.0	18.1	0.9	79.4	14.9	2.3	3.4
Cyclopropylamine	8	79.0	20.0	1.0	75.5	12.4	2.9	9.2
	12	79.1	19.4	1.5	75.8	12.7	3.2	8.3
	16	79.3	19.3	1.4	75.1	13.2	3.6	8.1
	30	79.6	19.1	1.3	76.5	14.7	2.6	6.2
	45	80.8	18.1	1.1	79.0	14.8	2.3	3.9
	60	81.2	17.3	1.5	80.1	14.6	2.2	3.1

DOI: 10.1002/ppap.200900131

synthesis. The subsequent reactions of these free radicals with oxygen and water, when exposed to ambient atmosphere, lead to the incorporation of oxygen-based functionalities in the PPF. The mechanisms of such PPF post-growth oxidation processes have extensively been studied.[35,40,62–64] The oxygen concentration in the as-deposited samples is lower than in the TFBA-derivatized ones since the former were analyzed immediately after synthesis, thus limiting the ageing effect. In contrast, the latter were let 40 h under TFBA atmosphere in which water is released during the derivatization reaction (Scheme 1). We also observe a decrease in the nitrogen content of the samples after the derivatization of the primary amines. This is explained by the incorporation of carbon, fluorine, and oxygen atoms in the PPF following the reaction between TFBA and the primary amine functionalities.

Figure 2b shows the evolution of $\%NH_2$ as a function of P_{mean}. In both systems, $\%NH_2$ decreases with growing P_{mean} as a result of the intensification of the precursor fragmentation in the plasma. Similarly to the precursor mass signal in the plasma (Figure 2a), $\%NH_2$ exhibits for both systems a critical P_{mean} value around 30 W (P^c_{mean}). For $P_{mean} > P^c_{mean}$, allylamine- and cyclopropylamine-based PPF have similar $\%NH_2$ whereas for $P_{mean} < P^c_{mean}$, PPF synthesized at the same P_{mean} contain a larger $\%NH_2$ with cyclopropylamine as the precursor. This is in full consistency with the mass spectrometry measurements indicating that cyclopropylamine is less fragmented in the plasma so that primary amine functionalities are more efficiently incorporated in the PPF. Interestingly enough, the process efficiency, that is, $[NH_2]/[C]$, is similar for both precursors.

Since the NH_2 groups have to be retained on the precursor hydrocarboned backbone to be efficiently incorporated in the PPF, the strength of the precursor C–N bond appears to be a key parameter to be considered. In order to validate this assumption, the C–N bond stability is hereafter theoretically explored with the help of DFT calculations. To do so, the enthalpies of reaction leading to C–N, C–C, and C–H bond breaking in allylamine and cyclopropylamine have been estimated and compared. Since the intensity of the ammonia signal (always much higher than the peak at m/z 16) is similar to the intensity of the peak at m/z 41 (characteristic signal of the hydrocarboned part of the precursor) in allylamine discharges, we have also investigated another breaking mechanism of the C–N bond involving the addition reaction of hydrogen on the nitrogen atom of the precursors.

Theoretical Part

Methodology

DFT calculations have been performed to optimize the geometries of the precursors and their fragments and to estimate the enthalpies of reaction associated to selected fragmentation pathways of the precursors. We have selected the B3LYP exchange-correlation functional with the 6-311++G (3df, 3pd) basis set which has been reported to provide a reliable description of homolytic bond breaking.[65–68] DFT calculations on radical systems are carried out within an unrestricted scheme instead of the restricted open-shell formalism;[69] we have checked that spin contamination is weak in all cases. All calculations have been performed using the Gaussian03 package.

Since the activation energy and enthalpy of reaction are almost equivalent for bond dissociation processes,[65–67,70] the latter has been estimated by simply calculating the energy difference between the reactants and the products. The enthalpy of reaction $\Delta H^o_r(T)$ is indistinctly called "heat of reaction" or "bond dissociation energy" (BDE). The term "classical BDE" (D_e) is used to define the difference in electronic energy between the products and reactants without including the zero-point energy and enthalpic contributions. The following relationship holds between the heat of formation and the classical BDE.

$$\Delta H^o_r(T) = D_e + \Delta ZPE + \Delta H_{trans} + \Delta H_{rot} + \Delta H_{vib} - RT \qquad (4)$$

where ΔZPE is the difference of zero-point energy between the products and reactants. ΔH_{trans}, ΔH_{rot}, and ΔH_{vib} are the contributions from translational, rotational, and vibrational degrees of freedom, respectively, to the enthalpy of reaction, as computed from statistical thermodynamics on the basis of the equilibrium structures. The vibrational frequencies are calculated within the harmonic oscillator approximation. No scaling factors are considered for the vibrational frequencies and the ZPE correction since the basis set used in conjunction with B3LYP requires a rescaling below 1%.[67,71] The BDE values are obtained here at 298 K.

Results and Discussion

Figure 3 reports the calculated enthalpies of reaction associated to allylamine initial fragmentations. The energies required to break the precursor chemical bonds range between 2.7 and 7.3 eV. The calculations suggest that the easiest reaction taking place in the plasma leads to the formation of allyl and NH_2 radicals as a result of the C–N bond dissociation. This is rationalized by the high stability of the allyl radical provided by the electron delocalization within the fragment. The NH_2 chemical group is thus easily removed from the hydrocarbon-based backbone of the precursor. For C–H bond breaking, the reaction requiring 3.2 eV is favored with respect to the others since the produced nitrogen-based fragment is stabilized by both the adjacent double bond and the nitrogen electronic doublet.

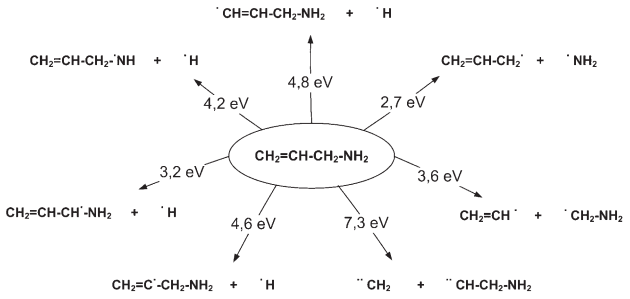

Figure 3. DFT-calculated reaction enthalpies associated to allylamine initial fragmentations.

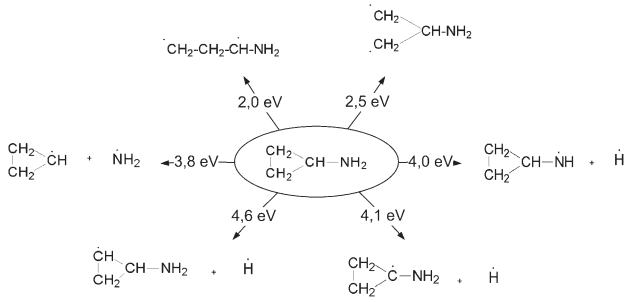

Figure 4. DFT-calculated reaction enthalpies associated to cyclopropylamine initial fragmentations.

As expected, the C–C bond breaking requires less energy than the C=C bond breaking since a smaller electronic density is involved. Figure 4 presents the reaction enthalpies associated to cyclopropylamine initial fragmentations. It turns out from the calculations that the reactions leading to the opening of the cyclopropylamine ring structure are the most likely to occur (with enthalpies of reaction of 2.0 and 2.5 eV, respectively). The two reactions do not involve any precursor fragmentation and generate activated (biradical) chemical species that retain the chemical group of interest (NH_2). The other reactions which entail the formation of NH_2 and H radicals require at least 3.8 eV. The predicted homolytic bond dissociation in cyclopropylamine is supported by a previous experimental work which has also underlined the loss of the cyclopropylamine cyclic structure, in that case when ionized via EI, and its rearrangement into a more stable opened conformation.[72] When taking an explicit account of entropic effects,[73] the results show a systematic decrease of ≈0.5 eV with respect to the calculated enthalpies of reaction, following the rise in entropy. Entropic effects do not thus modify the previous conclusions.

We now address at a theoretical level why ammonia (NH_3) is produced in a larger amount in allylamine plasmas compared to cyclopropylamine ones. The production of ammonia in the plasma implies hydrogen addition and/or transposition to the nitrogen of the precursors. According to

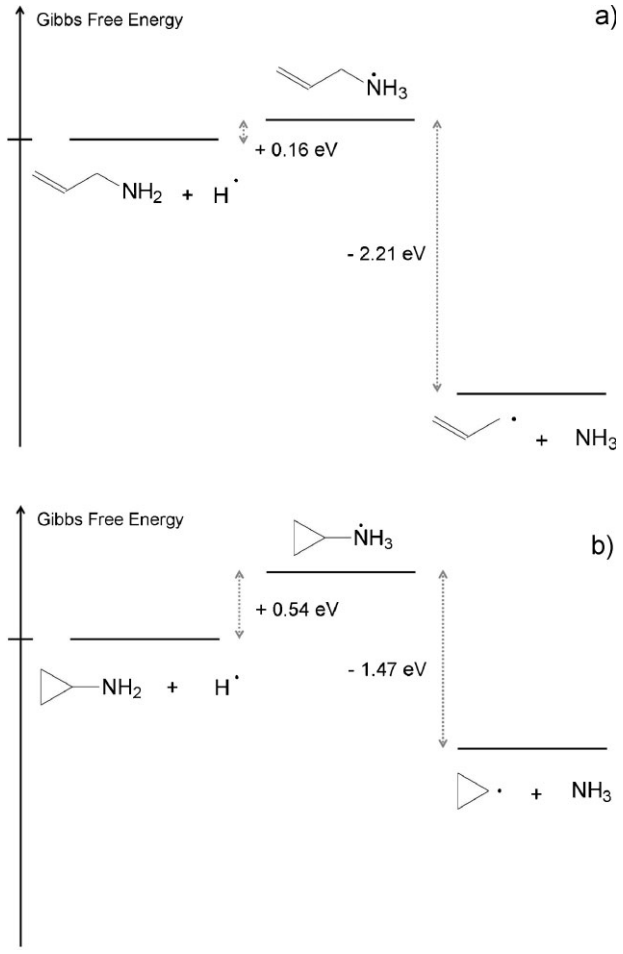

Figure 5. Gibbs free energy diagram for the addition reaction of hydrogen on the precursor nitrogen atom followed by C–N bond breaking for a) allylamine and b) cyclopropylamine.

a recent work on radiolyzed media, free radicals can be important sources of molecular fragmentation.[74] Since allylamine and cyclopropylamine plasmas are rich in hydrogen (see Figure 1c–f), as experimentally observed by mass spectrometry, we focused on a C–N bond breaking activated by the addition reaction of hydrogen on the nitrogen atom of the precursors. The calculated Gibbs free energies show that the formation of the reaction intermediate requires a barrier of 0.16 eV for allylamine while this value is three times larger for cyclopropylamine (0.54 eV), see Figure 5. Since no energy is fed into these reactions via electron collisions, these barriers introduce a clear selectivity between the two precursors. Following hydrogen addition, the C–N bond breaking in the reaction intermediate is in both cases exothermic and hence thermodynamically favored. The lower barrier calculated for allylamine upon hydrogen addition can thus explain the larger amount of ammonia produced in this plasma. Although the majority of precursor fragmentation

DOI: 10.1002/ppap.200900131

reactions arise from EI collisions in the plasma, our theoretical calculations indicate that bond breaking can also result from chemical reactions such as hydrogen addition. The ease of NH_3 loss from allylamine within such a reaction scheme is another element explaining the lower $\%NH_2$ compared to cyclopropylamine PPF.

The larger amount of nitrogen (i.e., a larger amount of nitrogen-based functionalities including, in addition to amines, imines, and nitriles) in allylamine compared to cyclopropylamine PPF suggested by XPS (see Table 2) may be rationalized by the fact that the nitrogen of the precursors is lost via the C–N bond dissociation, leading to the formation of either NH_X species or, following multi-step processes, molecular nitrogen. The presence of N_2 in the plasmas has been supported by optical emission spectroscopy via the identification of its second positive system (data not shown). The production of N_2 in the discharges should thus govern the overall PPF nitrogen content since NH_X species, and particularly NH_3, are produced in a larger amount in allylamine plasmas. When comparing the allylamine and the cyclopropylamine plasma chemistries as a function of P_{mean}, according to the intensity ratio between the mass signal at m/z 17 (ammonia) and m/z 28 (including N_2), the values of I^{17}/I^{28} are found to be sensitively lower for cyclopropylamine- than for allylamine-based plasmas, which seems to confirm the larger production of molecular nitrogen in cyclopropylamine discharges. However, it is important to point out that the intensity of the mass signal at m/z 28 is quite close in both types of plasmas when considering similar P_{mean}. Due to the different fragmentation patterns of the precursors in the plasma, as suggested by the presented mass spectra, this observation likely hides different isobaric contributions between allylamine plasmas and cyclopropylamine ones. One way to confirm that N_2 is produced in a larger amount in cyclopropylamine discharges would be to employ methods more selective than mass spectrometry toward the detection and quantification of the plasma species, such as laser-induced fluorescence (LIF).

Conclusion

In this work, pulsed plasma polymerization of two isomeric primary amine-based precursors, namely allylamine and cyclopropylamine, has been investigated to study the influence of the precursor chemical structure on the process selectivity toward primary amine groups. The precursor fragmentation patterns in the plasma have been examined by RGA mass spectrometry while the primary amine content of the corresponding thin films has been evaluated by a combination of chemical derivatization reaction and XPS. The influence of the mean power injected in the plasma has been studied for both systems. The results show an amplification of the precursor fragmentation in the plasma when the mean power dissipated in the discharge increases while the primary amine content incorporated in the formed PPF gets lowered. A critical value of mean power (≈30 W) has been determined. Below this value, different behaviors are observed as a function of the precursor chemical structure, cyclopropylamine being less plasma-fragmented than allylamine. As a result, in this mean power range, cyclopropylamine PPF yields a higher primary amine content. This difference between cyclopropylamine and allylamine discharges has been correlated to internal bond energies of the precursors, as calculated at the DFT level. The theoretical approach also indicates that some plasma species (e.g., NH_3) are not only the result of precursor fragmentation but also require chemical reactions such as hydrogen addition to be produced. The lower fragmentation of cyclopropylamine in the plasma is explained by a preferential opening of the ring structure whose C–C bonds are characterized by the lowest BDEs compared to the energy required for C–N or C–H bond breaking. The activation of cyclopropylamine through EI collisions can thus occur without fragmentation reactions. The chemical group of interest is then retained on the precursor hydrocarboned backbone, so that the incorporation of the primary amine group in the films is more efficient than for allylamine which is preferentially activated by the C–N bond breaking and hence by the loss of the precursor functional group. The full consistency between the experimental and theoretical results opens the way for a theoretical screening of precursors aiming at the optimization of the PPF functionalization.

Acknowledgements: This work is supported by the *Fonds pour la Formation à la Recherche dans l'Industrie et dans l'Agriculture* (F.R.I.A.) and the *Belgian Government* through the *Pôle d'Attraction Interuniversitaire* (PAI, P6/08, "Plasma-Surface Interaction", Ψ). J. C. is a research fellow of the Fonds National de la Recherche Scientifique (F.N.R.S.).

Received: August 7, 2009; Revised: October 22, 2009; Accepted: October 23, 2009; DOI: 10.1002/ppap.200900131

Keywords: chemical derivatization; density functional theory (DFT); films; mass spectrometry; primary amines; pulsed plasma polymerization; X-ray photoelectron spectroscopy (XPS)

[1] H. Biederman, Y. Osada, *Plasma Technology, Vol. 3 – Plasma Polymerization Processes*, L. Holland, Ed., Elsevier Science Publishers, Amsterdam 1992, p. 4.
[2] H. Yasuda, *Plasma Polymerization*, Academic Press, Orlando 1985.

[3] A. M. Wrobel, M. R. Wertheimer, in: *Plasma Deposition, Treatment, and Etching of Polymers*, R. d'Agostino, Ed., Academic Press, San Diego 1990, Ch. 3.
[4] B. D. Beake, S. Zheng, M. R. Alexander, *J. Mater. Sci.* **2002**, *37*, 3821.
[5] R. Prikryl, V. Cech, L. Zajickova, J. Vanek, S. Behzadi, F. R. Jones, *Surf. Coat. Technol.* **2005**, *200*, 468.
[6] N. Inagaki, *Plasma Surface Modification and Plasma Polymerization*, Technomic Publishing, Lancaster 1996, Ch. 5.
[7] A. Grill, *Cold Plasma in Materials Fabrication – From Fundamentals to Applications*, IEEE Press, New York 1994.
[8] L. O'Toole, A. J. Beck, A. P. Ameen, F. R. Jones, R. D. Short, *J. Chem. Soc. Faraday Trans.* **1995**, *91*, 3907.
[9] M. R. Alexander, F. R. Jones, R. D. Short, *Plasmas Polym.* **1997**, *2*, 277.
[10] L. O'Toole, C. A. Mayhew, R. D. Short, *J. Chem. Soc. Faraday Trans.* **1997**, *93*, 1961.
[11] A. J. Beck, S. Candan, R. M. France, F. R. Jones, R. D. Short, *Plasmas Polym.* **1998**, *3*, 97.
[12] A. J. Beck, F. R. Jones, R. D. Short, *J. Chem. Soc. Faraday Trans.* **1998**, *94*, 559.
[13] S. Candan, A. J. Beck, L. O'Toole, R. D. Short, A. Goodyear, N. St J. Braithwaite, *Phys. Chem. Chem. Phys.* **1999**, *1*, 3117.
[14] D. B. Haddow, R. M. France, R. D. Short, J. W. Bradley, D. Barton, *Langmuir* **2000**, *16*, 5654.
[15] A. J. Beck, S. Candan, R. D. Short, A. Goodyear, N. St J. Braithwaite, *J. Phys. Chem. B* **2001**, *105*, 5730.
[16] C. R. Savage, R. B. Timmons, J. W. Lin, *Chem. Mater.* **1991**, *3*, 575.
[17] R. B. Timmons, A. J. Griggs, in: *Plasma Polymer Films*, H. Biederman, Ed., Imperial College Press, London 2004, Ch. 6.
[18] R. Förch, Z. Zhang, W. Knoll, *Plasma Processes Polym.* **2005**, *2*, 351.
[19] A. Harsch, J. Calderon, R. B. Timmons, G. W. Gross, *J. Neurosci. Methods* **2000**, *98*, 135.
[20] H. Schönherr, M. T. van Os, R. Förch, R. B. Timmons, W. Knoll, J. Vancso, *Chem. Mater.* **2000**, *12*, 3689.
[21] Z. Zhang, Q. Chen, W. Knoll, R. Foerch, R. Holcomb, D. Roitman, *Macromolecules* **2003**, *36*, 7689.
[22] A. Choukourov, H. Biederman, D. Slavinska, L. Hanley, A. Grinevich, H. Boldyryeva, A. Mackova, *J. Phys. Chem. B* **2005**, *109*, 23086.
[23] L. Denis, D. Cossement, T. Godfroid, F. Renaux, C. Bittencourt, R. Snyders, M. Hecq, *Plasma Processes Polym.* **2009**, *6*, 199.
[24] R. C. Ruaan, T. H. Wu, S. H. Chen, J. Y. Lai, *J. Membr. Sci.* **1998**, *138*, 213.
[25] I. Gancarz, G. Pozniak, M. Bryjak, W. Tylus, *Eur. Polym. J.* **2002**, *38*, 1937.
[26] P. Hamerli, T. Weigel, T. Groth, D. Paul, *Biomaterials* **2003**, *24*, 3989.
[27] G. Oye, V. Roucoules, A. M. Cameron, L. J. Oates, N. R. Cameron, P. G. Steel, J. P. S. Badyal, B. G. Davis, D. Coe, R. Cox, *Langmuir* **2002**, *18*, 8996.
[28] G. Oye, V. Roucoules, L. J. Oates, A. M. Cameron, N. R. Cameron, P. G. Steel, J. P. S. Badyal, B. G. Davis, D. M. Coe, R. A. Cox, *J. Phys. Chem. B* **2003**, *107*, 3496.
[29] Q. Chen, L. Dai, M. Gao, S. Huang, A. Mau, *J. Phys. Chem. B* **2001**, *105*, 618.
[30] L. Dai, H. A. W. St John, J. Bi, P. Zientek, R. C. Chatelier, H. J. Griesser, *Surf. Interface Anal.* **2000**, *29*, 46.
[31] Q. Chen, R. Förch, W. Knoll, *Chem. Mater.* **2004**, *16*, 614.
[32] Z. Zhang, W. Knoll, R. Förch, *Surf. Coat. Technol.* **2005**, *200*, 993.
[33] R. Förch, A. N. Chifen, A. Bousquet, H. L. Khor, M. Jungblut, L.-Q. Chu, Z. Zhang, I. Osey-Mensah, E.-K. Sinner, W. Knoll, *Chem. Vap. Deposition* **2007**, *13*, 280.
[34] T. B. Ren, T. Weigel, T. Groth, A. Lendlein, *J. Biomed. Mater. Res., Part A* **2008**, *86A*, 209.
[35] T. R. Gengenbach, R. C. Chatelier, H. J. Griesser, *Surf. Interface Anal.* **1996**, *24*, 271.
[36] Y. Martin, D. Boutin, P. Vermette, *Thin Solid Films* **2007**, *515*, 6844.
[37] K. Vasilev, L. Britcher, A. Casanal, H. J. Griesser, *J. Phys. Chem. B* **2008**, *112*, 10915.
[38] J. Kim, D. Jung, Y. Park, Y. Kim, D. W. Moon, T. G. Lee, *Appl. Surf. Sci.* **2007**, *253*, 4112.
[39] A. Choukourov, H. Biederman, D. Slavinska, M. Trchova, A. Hollander, *Surf. Coat. Technol.* **2003**, *174*, 863.
[40] T. R. Gengenbach, H. J. Griesser, *J. Polym. Sci. Pol. Chem.* **1999**, *37*, 2191.
[41] F. Fally, C. Doneux, J. Riga, J. J. Verbist, *J. Appl. Polym. Sci.* **1995**, *56*, 597.
[42] A. G. Shard, J. D. Whittle, A. J. Beck, P. N. Brookes, N. A. Bullet, R. A. Talib, A. Mistry, D. Barton, S. L. McArthur, *J. Phys. Chem. B* **2004**, *108*, 12472.
[43] V. Krishnamurthy, I. L. Kamel, *J. Polym. Sci. Pol. Chem.* **1989**, *27*, 1211.
[44] M. Tatoulian, F. Bretagnol, F. Arefi-Khonsari, J. Amouroux, O. Bouloussa, F. Rondelez, A. J. Paul, R. Mitchell, *Plasma Processes Polym.* **2005**, *2*, 38.
[45] U. Oran, S. Swaraj, A. Lippitz, W. E. S. Unger, *Plasma Processes Polym.* **2006**, *3*, 288.
[46] S. Igarashi, A. N. Itakura, M. Toda, M. Kitajima, L. Chu, A. N. Chifen, R. Förch, R. Berger, *Sens. Actuators, B: Chem.* **2006**, *117*, 43.
[47] M. Lejeune, F. Bretagnol, G. Ceccone, P. Colpo, F. Rossi, *Surf. Coat. Technol.* **2006**, *200*, 5902.
[48] G. S. Malkov, I. T. Martin, W. B. Schwisow, J. P. Chandler, B. T. Wickes, L. J. Gamble, D. G. Castner, E. R. Fisher, *Plasma Processes Polym.* **2008**, *5*, 129.
[49] M. J. Vasile, G. Smolinsky, *Int. J. Mass Spectrom.* **1976**, *21*, 263.
[50] R. Manory, A. Grill, U. Carmi, R. Avni, *Plasma Chem. Plasma Process.* **1983**, *3*, 235.
[51] J. H. Scofield, *J. Electron Spectrosc. Relat. Phenom.* **1976**, *8*, 129.
[52] *Surface Analysis – The Principal Techniques*, J. C. Vickerman, Ed., John Wiley & Sons Ltd, Chichester 1997, Ch. 3.
[53] G. C. Smith, in: *Handbook of Surface and Interface Analysis: Methods for Problem-Solving*, J. C. Rivière, S. Myhra, Eds., Marcel Dekker, New York 1998, Ch. 5.
[54] C. D. Batich, *Appl. Surf. Sci.* **1988**, *32*, 57.
[55] A. Chilkoti, B. D. Ratner, D. Briggs, *Chem. Mater.* **1991**, *3*, 51.
[56] S. Pan, D. G. Castner, B. D. Ratner, *Langmuir* **1998**, *14*, 3545.
[57] P. Favia, M. V. Stendardo, R. d'Agostino, *Plasmas Polym.* **1996**, *1*, 91.
[58] G. Cicala, M. Creatore, P. Favia, R. Lamendola, R. d'Agostino, *Appl. Phys. Lett.* **1999**, *75*, 37.
[59] I. Losito, E. De Giglio, N. Cioffi, C. Malitesta, *J. Mater. Chem.* **2001**, *11*, 1812.
[60] A. A. Meyer-Plath, K. Schröder, B. Finke, A. Ohl, *Vacuum* **2003**, *71*, 391.
[61] F. Truica-Marasescu, M. R. Wertheimer, *Plasma Processes Polym.* **2008**, *5*, 44.
[62] T. R. Gengenbach, Z. R. Vasic, R. C. Chatelier, H. J. Griesser, *J. Polym. Sci. Pol. Chem.* **1994**, *32*, 1399.

DOI: 10.1002/ppap.200900131

[63] T. R. Gengenbach, R. C. Chatelier, H. J. Griesser, *Surf. Interface Anal.* **1996**, *24*, 611.
[64] T. R. Gengenbach, Z. R. Vasic, S. Li, R. C. Chatelier, H. J. Griesser, *Plasmas Polym.* **1997**, *2*, 91.
[65] T. B. Casserly, K. K. Gleason, *Plasma Processes Polym.* **2005**, *2*, 669.
[66] S. Böhm, O. Exner, *J. Comput. Chem.* **2006**, *27*, 571.
[67] M. P. Badenes, C. J. Cobos, *J. Mol. Struct.: THEOCHEM* **2007**, *814*, 51.
[68] J. Tirado-Rives, W. L. Jorgensen, *J. Chem. Theory Comput.* **2008**, *4*, 297.
[69] J. A. Pople, P. M. W. Gill, N. C. Handy, *Int. J. Quantum Chem.* **1995**, *56*, 3003.
[70] P. Marsal, M. Roche, P. Tordo, P. de Sainte Claire, *J. Phys. Chem. A* **1999**, *103*, 2899.
[71] A. P. Scott, L. Radom, *J. Phys. Chem.* **1996**, *100*, 16502.
[72] G. Bouchoux, C. Alcaraz, O. Dutuit, M. T. Nguyen, *J. Am. Chem. Soc.* **1998**, *120*, 152.
[73] *Molecular Thermodynamics*, D. A. McQuarrie, J. D. Simon, Eds., University Science Books, Sausalito 1999.
[74] D. Kozlowski, P. Marsal, M. Steel, R. Mokrini, J.-L. Duroux, R. Lazzaroni, P. Trouillas, *Radiat. Res.* **2007**, *168*, 243.